Effect of *N*-cetyl-*N,N,N*-trimethylammonium bromide and orthophenylenediamine on the corrosion inhibition of carbon steel in 1 mol/L HCl

B. Ramesh Babu, A.K. Parande, and P.L. Ramasamy

Abstract: Inhibition studies of *N*-cetyl-*N,N,N*-trimethylammonium bromide (CTAB) and orthophenylenediamine (OPD) have shown that they were effective inhibitors of corrosion of carbon steel in HCl. The inhibitive behaviour of OPD with CTAB on the corrosion of carbon steel in 1 mol/L HCl was studied by gravimetric weight loss, potentiodynamic polarization, and electrochemical impedance measurements. Inhibition efficiency (IE) was found to increase with the increase in concentration of CTAB and it was also found that CTAB was effective only when used above a concentration of 100 mmol/L. Furthermore, the addition of 20 mmol/L of OPD to CTAB slightly increased the IE. The adsorption of these compounds on carbon steel in 1 mol/L HCl obeyed Langmuir's adsorption isotherm. These inhibitors reduced the permeation current. The IE was observed as high for 200 mmol/L of CTAB with 20 mmol/L of OPD in all the techniques studied. Scanning electron microscopy clearly showed that the inhibition was due to a polymolecular film formed by the physical adsorption of the inhibitor on the metal surface.

Key words: carbon steel, corrosion, inhibitors, impedance, potentiodynamic polarization.

Résumé : Des études d'inhibition ont permis de montrer que le bromure de *N*-cétyl-*N,N,N*-triméthylammonium (BCTA) et de l'orthophénylènediamine (OPD) sont des inhibiteurs efficaces de corrosion de l'acier au carbone dans l'acide chlorhydrique. On a étudié le comportement inhibiteur de l'OPD en présence de BCTA sur l'inhibition de la corrosion de l'acier au carbone dans de l'acide chlorhydrique 1 mol/L à l'aide de mesures gravimétrique, galvanostatique et d'impédance. On a trouvé que l'efficacité de l'inhibition (EI) augmente avec une augmentation de la concentration du BCTA et on a aussi observé que le BCTA n'est efficace que lorsque sa concentration est supérieure à 100 mmol/L. De plus, l'addition de 20 mmol/L d'OPD au BCTA augmente aussi l'efficacité de l'inhibition. L'adsorption de ces composés sur de l'acier au carbone dans de l'acide chlorhydrique 1 mol/L obéit à une isotherme d'adsorption de Langmuir. Ces inhibiteurs réduisent le courant de perméation. Dans toutes les techniques étudiées, on a observé une efficacité d'inhibition jusqu'à des valeurs de 200 mmol/L de BCTA avec 20 mmol/L d'OPD. La microscopie électronique à balayage a montré clairement que l'inhibition est due à un film polymoléculaire qui se forme par une adsorption physique de l'inhibiteur sur la surface métallique.

Mots clés : acier au carbone, corrosion, inhibiteurs, impédance, galvanostatique, polarisation.

Introduction

Corrosion of steel in acidic solutions has practical importance (1–7). For example, corrosion is of significant concern in the acid pickling of iron and steel, chemical cleaning of scale in metallurgy and other industries, and in oil recovery and other petrochemical processes. One of the most important means of corrosion protection is the use of organic inhibitors (8–15). Surfactants are used as corrosion inhibitors. These surfactants can be used either alone or in mixtures with other compounds. *N*-Cetyl-*N,N,N*-trimethylammonium bromide (CTAB), a cationic surfactant, has been used in controlling the corrosion of carbon steel in an aqueous solution containing chlorine ions (16). Orthophenylenediamine

(OPD), a nonionic surfactant, has been used as inhibitor for the corrosion of carbon steel in HCl (17). Several studies of surfactant mixtures focused on synergism in both micelle and monolayer formation at the air–water interface (18, 19). Surfactants have been used as corrosion inhibitors either alone (20) or in combination with other compounds to improve their performance as inhibitors (21, 22). CTAB is a cationic surfactant, whereas OPD is a nonionic surfactant. The aim of the present investigation was to study the combined effect of cationic (CTAB) and nonionic (OPD) surfactants on the corrosion inhibition of carbon steel in 1 mol/L HCl. The present work was carried out to investigate the following: (*i*) the inhibition effect of CTAB alone in the corrosion of carbon steel in 1 mol/L HCl and (*ii*) the combined

inhibition effect of OPD with CTAB in the corrosion of carbon steel in 1 mol/L HCl. The results are reported and discussed.

Experimental

Materials used

Carbon steel specimens

The chemical composition (wt%) of the carbon steel used in these tests was C 0.07%, P 0.08%, Mn 0.034%, S 0.04%, with the remainder being iron. Test specimens of size 5 cm × 3 cm × 0.2 cm were used for gravimetric studies. The specimens, embedded in epoxy resins with an exposed area of 1 cm^2 were used for potentiodynamic and impedance measurements. The specimens were polished with different grades of emery paper and degreased with trichloroethylene before use.

Reagents

AR chemicals of HCl, orthophynylenediamine, and *N*-cetyl-*N*,*N*,*N*-trimethyl ammonium bromide were used for this study. Table 1 shows the structures of CTAB and OPD.

Techniques adopted

Gravimetric test

The weighed specimens were exposed in 150 mL of 1 mol/L HCl containing different concentrations of inhibitor for a period of 3 days. After 3 days of exposure, the specimens were removed, washed, dried, and weighed. The experiments were conducted at 30 ± 1 °C using a temperature control bath (Siskin Juloba, India). The inhibition efficiency (IE) was calculated using the formula,

[1] $IE = 100 \left[1 - W_2 / W_1 \right]\%$

where W_1 = the initial weight of the specimen and W_2 = final weight of the specimen.

Potentiodynamic polarization

A three-electrode cell assembly, consisting of a carbon steel electrode with an exposed area of 1 cm^2 as working electrode, a saturated calomel electrode as reference electrode, and a platinum foil as counter electrode, was used for potentiodynamic polarization studies. The scan range was –650 to –400 mV; the scan rate was 1 mV sec^{-1} and an Electrochemical Analyzer (IM6) was used to generate the scans. From the polarization curves, b_a, b_c, E_{corr}, and I_{corr} values were calculated for carbon steel in uninhibited and inhibited hydrochloric acid. The corrosion IE was calculated using the equation,
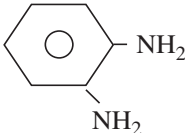
[2] $IE = 100 \left[1 - I_{corr(W)} / I_{corr(WO)} \right]\%$

where $I_{corr\ (W)}$ = corrosion current in the presence of inhibitor and $I_{corr\ (WO)}$ = corrosion current without inhibitor.

Electrochemical impedance spectroscopy

Electrochemical impedance spectroscopy (EIS) measurements were carried out using the three-electrode cell assembly, as mentioned in polarization studies, after 15 min of immersion. Experiments were carried out using Solartron SI 1287 in the frequency range of 60 KHz to 10 MHz. The ap-

Table 1. Structures of CTAB and OPD.

Compound	Structure
N-Cetyl-*N*,*N*,*N*-trimethyl ammonium bromide	$CH_3(CH_2)_{15}N^+ (CH_3)_3$ Br
Orthophenylenediamine (OPD)	

plied sinusoidal wave voltage was 5 mV. Nyquist plots were drawn from these results. From the plots, values of polarization resistance, R_p, were calculated. After substituting R_p values in the Stern–Geary equation, the corrosion rate was calculated using,

[3] $I_{corr} = \dfrac{b_a b_c}{2.303 (b_a + b_c)} \left(\dfrac{1}{R_p} \right)$

The IE was calculated using the value of I_{corr} for various systems studied.

Hydrogen permeation studies

The hydrogen permeation studies were carried out using a Devanathan and Stachurski two-compartment cell as described elsewhere (23). Permeation current was obtained for a concentration of 1 mol/L HCl, 1 mol/L HCl with 200 mmol/L CTAB, and 200 mmol/L CTAB and 20 mmol/L OPD in 1 mol/L HCl.

Scanning electron microscopy

Micrographs were made of carbon steel specimens using an Hitachi Model-S-3000 H. Carbon steel specimens of size 1 cm^2 were dipped in 1 mol/L HCl with and without inhibitors for surface analysis.
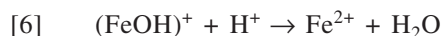
Results and discussion
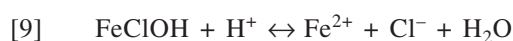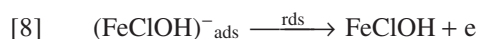
Mechanism of corrosion inhibition

It has been hypothesized that the mechanism of iron dissolution occurs in two consecutive steps and involves the participation of a species $(FeOH)_{ads}$ as shown here,

[4] $Fe + H_2O \leftrightarrow (FeOH)_{ads} + H^+ + e$

[5] $Fe(OH)_{ads} \xrightarrow{\text{rds}} (FeOH)^+ + e$
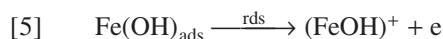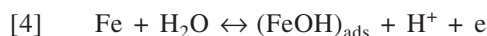
where rds refers to rate determining step, and
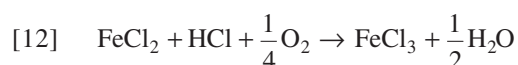
[6] $(FeOH)^+ + H^+ \rightarrow Fe^{2+} + H_2O$

The dissolution of iron in HCl solution has been studied extensively. One of the mechanisms of breakdown of passivity involves the diffusion of Cl$^-$ through the protective oxide layer. The reaction sequence is supposed to involve the following steps,

[7] $Fe + Cl^- + H_2O \leftrightarrow (FeClOH)^-_{ads} + H^+ + e^-$

[8] $(FeClOH)^-_{ads} \xrightarrow{\text{rds}} FeClOH + e$

[9] $FeClOH + H^+ \leftrightarrow Fe^{2+} + Cl^- + H_2O$

where $(FeClOH)^-_{ads}$ was treated as per Langmuir's isotherm.

It is well-known that the passive film consists of hydrated iron oxides, $Fe_2O_3 \cdot H_2O$. When the aggressive Cl^- anion attacks the passive film, the Cl^- ions tend to diffuse towards the metal (they meet with bound water molecules, which are the cementing elements of the passive layer) and form chloride-containing iron complexes, which in turn increase the dissolution rate. It has also been confirmed that the presence of chlorides accelerates the formation of corrosion products because of the corresponding cyclic processes of rusting.

In the case of chlorides, the process (Fig. 1) takes place in three phases, reactions [10–12], with the net formation of ferric hydroxide iron with water and oxygen in the presence of acid.

[10] $FeCl_3 + 3H_2O \rightarrow Fe(OH)_3 + 3HCl$

[11] $Fe + 2HCl \rightarrow FeCl_2 + H_2$

[12] $FeCl_2 + HCl + \dfrac{1}{4}O_2 \rightarrow FeCl_3 + \dfrac{1}{2}H_2O$
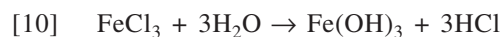
The circle of ongoing corrosion is closed, as the ferric chloride consumed in reaction [10] reappears in reaction [12]. The net reaction, which is the sum of reactions [10–12] is

[13] $Fe + 2.5H_2O + 0.25O_2 \rightarrow Fe(OH)_3 + H_2$
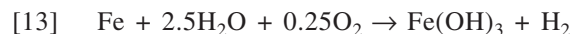
Inhibition efficiency by gravimetric method

The IE calculated for 50, 100, 150, 200, and 250 mmol/L concentrations of CTAB alone in 1 mol/L HCl and the addition of 20 mmol/L OPD with different concentrations of CTAB were reported in Table 2. From the table, it is seen that the IE increases from 50 to 200 mmol/L of CTAB alone and similarly from 50 to 200 mmol/L of CTAB with 20 mmol/L of OPD. The optimum concentration of CTAB and OPD was found to be 200 mmol/L. A further increase in inhibitor does not show any increase in the IE, and there is a decrease in IE at 250 mmol/L of CTAB both alone and with OPD.

Inhibition efficiency by potentiodynamic polarization

Figures 2 and 3 show the polarization curves for carbon steel in 1 mol/L HCl with and without inhibitors. The corrosion parameters such as b_a, b_c, E_{corr}, I_{corr}, and IE collected for 1 mol/L HCl containing different concentrations of CTAB with and without OPD were reported in Table 3. The addition of CTAB and OPD influence the b_c values with less potential difference. Similarly, the E_{corr} values are found to be little changed when compared with blank. This indicates that the studied compounds are of mixed type of inhibitor. From the table it was found that as the concentration of the inhibitor increased from 50 to 200 mmol/L, the IE increased markedly compared with using CTAB alone. The addition of OPD in different concentrations of CTAB increased IE, but no further improvement was found with the addition of OPD to 250 mmol/L CTAB.

Because CTAB has a long chain molecule, the surface coverage area, θ, also leads to an increase in IE when used alone. Hence, it is a good inhibitor. The addition of OPD increases the IE to a lesser extent. The availability of an electron in the benzene ring in OPD and a nitrogen atom plays a
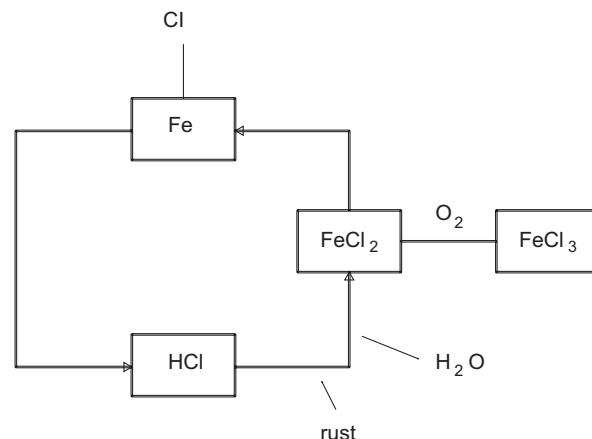
Fig. 1. Reaction of chloride with iron.

Table 2. Inhibition efficiencies (IE) of CTAB and OPD for the corrosion of carbon steel in 1 mol/L HCl as determined by the gravimetric method.

Inhibitor	CTAB concn. (mmol/L)	IE (%)
CTAB	50	60.4
	100	67.2
	150	78.6
	200	89.2
	250	85.6
CTAB and 20 mmol/L OPD	50	64.3
	100	72.5
	150	81.9
	200	92.3
	250	91.4

vital role in the adsorption of the inhibitor to the steel surface. The nitrogen atoms present in OPD enhance its efficiency. The combination of both has a synergistic effect.

The value of the anodic Tafel slope was reduced from 130 mV dec^{-1} to 110 mV dec^{-1}. The value of the cathodic Tafel slope was between 70 mV dec^{-1} and 60 mV dec^{-1}. These data show that the inhibitors, CTAB and OPD, inhibit the corrosion of carbon steel acting as mixed inhibitors.

## Electrochemical impedance spectroscopy (EIS) studies

AC impedance technique has been widely used as a tool in the investigation of the protective properties of organic inhibitors for metals. The technique is based on the measurement of the impedance of the double layer at the metal–solution interface. The charge transfer resistance, R_t, and the double layer capacitance, C_{dl}, are calculated by determining the equivalent electrical circuit of the metal–solution interface. In general for a corrosion system, the equivalent circuit diagram is as given in Fig. 4. C_{dl} is the double layer capacitance, R_t the charge transfer resistance, and R_s is the solution resistance.

The impedance of the circuit given in Fig. 4 can be calculated using,

[14] $Z = R_s + \dfrac{R_t}{1 + j\omega C_{dl} R_t}$

Table 3. Potentiodynamic polarization parameters for carbon steel in 1 mol/L HCl in the presence of inhibitors.

Inhibitor	CTAB Conc. (mmol/L)	E_{corr} (mV)	I_{corr} (mA cm^{-2})	b_a (mV dec^{-1})	b_c (mV dec^{-1})	IE (%)
Blank	—	−520	3.2	130	70	—
CTAB	50	−518	1.04	118	60	67.5
	100	−516	0.99	110	64	69.0
	150	−512	0.75	120	66	76.5
	200	−506	0.68	126	68	78.7
	250	−510	0.73	121	66	77.1
CTAB and 20mmol/L OPD	50	−516	0.89	120	64	72.1
	100	−512	0.67	118	66	79.0
	150	−504	0.54	126	67	83.1
	200	−498	0.48	128	72	85.0
	250	−500	0.52	124	66	83.7

Fig. 2. Polarization curves for carbon steel in blank and in different concentrations of CTAB. (*a*) Blank, (*b*) 50 mmol/L, (*c*) 100 mmol/L, (*d*) 150 mmol/L, (*e*) 200 mmol/L, and (*f*) 250 mmol/L C.
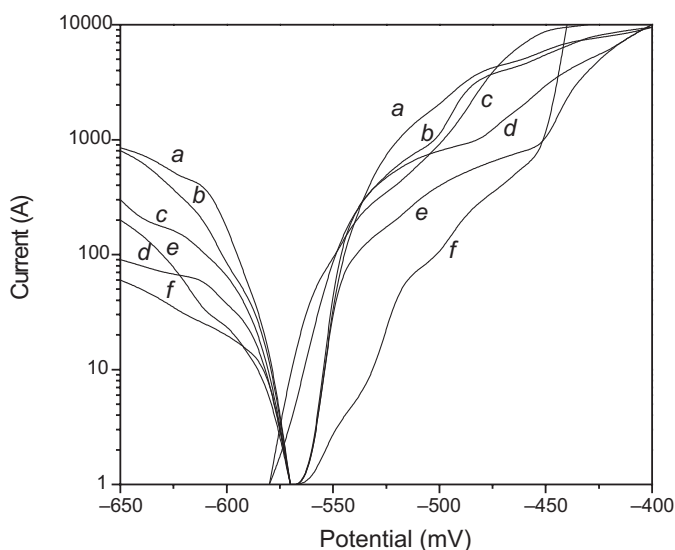
Fig. 3. Polarization curves for carbon steel in blank and in different concentrations of CTAB with OPD. (*a*) Blank, (*b*) 50 mmol/L CTAB and 20 mmol/L OPD, (*c*) 100 mmol/L CTAB and 20 mmol/L OPD, (*d*) 150 mmol/L CTAB and 20 mmol/L OPD, (*e*) 200 mmol/L CTAB and 20 mmol/L OPD, and (*f*) 250 mmol/L CTAB and 20 mmol/L OPD.
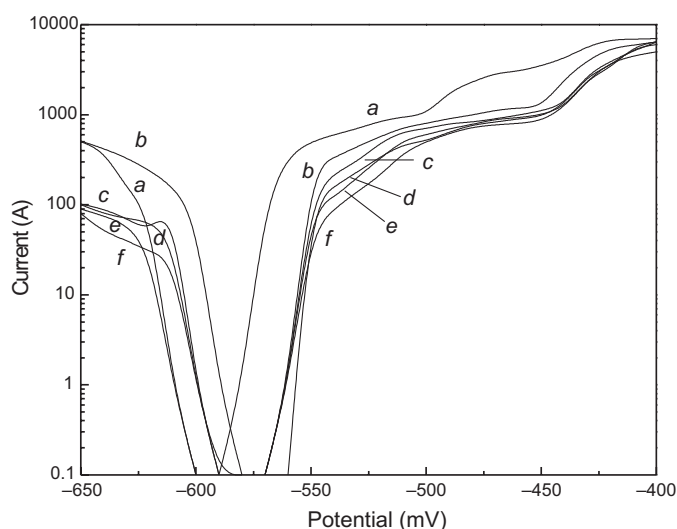
$$[15] \quad Z = R_s + \frac{R_t}{1 + \omega^2 C_{dl}^2 R_t^2} - \frac{j\omega C_{dl} R_t^2}{1 + \omega^2 C_{dl}^2 R_t^2}$$

where R_s is the solution resistance, R_t the charge transfer resistance, j is the imaginary unit ($\sqrt{-1}$), ω is the angular frequency ($\omega = 2\pi f$), and C_{dl} is the double layer capacitance. Equation [15] can be expressed as

$$[16] \quad Z = Z' - jZ''$$

where

$$[17] \quad Z = Z' - jZ''$$

$$[18] \quad Z' = R_s + \frac{R_t}{1 + \omega^2 C_{dl}^2 R_t^2}$$

Eliminating ω between eqs. [17] and [18] gives the following equation for a semicircle,

$$[19] \quad \left[Z' - \left(\frac{R_s + R_t}{2} \right) \right]^2 + (Z'')^2 = \left(\frac{R_t}{2} \right)^2$$

According to eq. [19], the experimental data should give a Nyquist plot in the shape of a semicircle. In a real corrosion system, semicircular Nyquist plots can be obtained only with a few metals, and most of the experimental plots deviate from a semicircle.
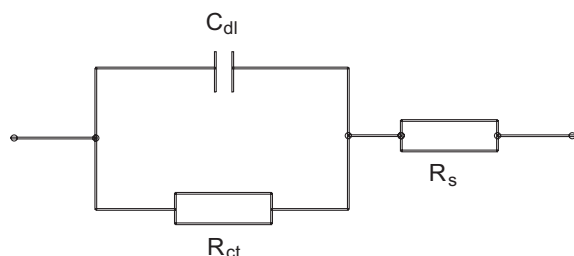
The value of R_t will be determined from the following equation,

$$[20] \quad I_{corr} = \frac{b_a b_c}{2.3 (b_a + b_c)} \frac{1}{R_t}$$

The values of C_{dl} and R_p derived from Nyquist plots, which have been shown in Fig. 5 for CTAB with and without OPD systems, were reported in Table 4.

Table 4. Impedance parameters for the corrosion of carbon steel in 1 mol/L HCl in the presence of inhibitors.

Inhibitor	CTAB Conc. (mmol/L)	R_P (Ω cm^2)	C_{dl} (μF cm^{-2})	I_{corr} (mA cm^{-2})
Blank	—	4.3	318	4.59
CTAB	50	13.7	154	1.34
	100	15.2	146	1.2
	150	17.8	133	1.08
	200	19.7	117	0.87
	250	20.1	114	0.89
CTAB and 20mmol/L OPD	50	14.2	144	1.28
	100	15.8	131	1.16
	150	18.5	125	1.04
	200	22.1	110	0.78
	250	21.8	113	0.84

Fig. 4. Equivalent circuit diagram for the corrosion system.

Fig. 5. Typical Nyquist plots for carbon steel in blank, CTAB, and OPD. (*a*) Blank, (*b*) 150 mmol/L CTAB, and (*c*) 150 mmol/L CTAB and 20 mmol/L OPD.
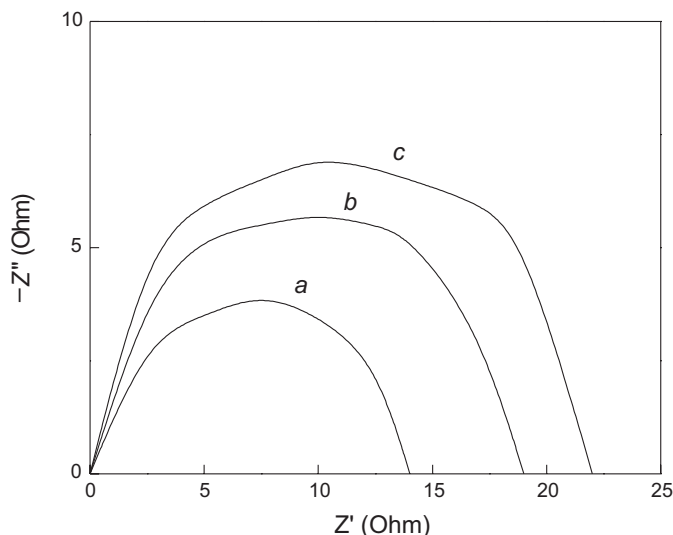

The C_{dl} value decreased with the addition of CTAB and it was further reduced by the addition of OPD. The data show that the greater the adsorption of inhibitor, the smaller C_{dl} values that were obtained. C_{dl} indirectly measures the water uptake by the passive film. From the data, 200 mmol/L of CTAB with 20 mmol/L of OPD showed the smallest values of C_{dl} when compared with other concentrations studied. This was explained by the presence of the cations present in the surfactant, which have better adsorption properties than a neutral surfactant.

The R_p value for blank was reported as 4.3 Ω cm^2. The addition of CTAB increased the R_p values by 4–5 times in different concentrations. Furthermore, the addition of 20 mmol/L of OPD with different concentrations of CTAB increased the R_p values from 14.2 to 22.1 Ω cm^2. This data showed that the greater the surface coverage of the adsorbed inhibitor, the greater R_p values that were obtained.

The I_{corr} value measured for blank was 4.59 mA cm^{-2}. The I_{corr} values were decreased drastically from 1.34 to 0.87 mA cm^{-2} for different concentrations of CTAB alone. The addition of OPD in CTAB decreased the I_{corr} values further. From the Table 4, the C_{dl} value for the blank was reported as 318 μF cm^{-2}.

Adsorption isotherm

The interaction between the inhibitors and the steel surface can be described by the adsorption isotherm. During corrosion inhibition of metals, the nature of the inhibitor on the corroding surface has been deduced in terms of the adsorption characteristics of the inhibitor. The adsorption of organic inhibitors at an electrolyte–electrode interface may take place through displacement of adsorbed water mole-
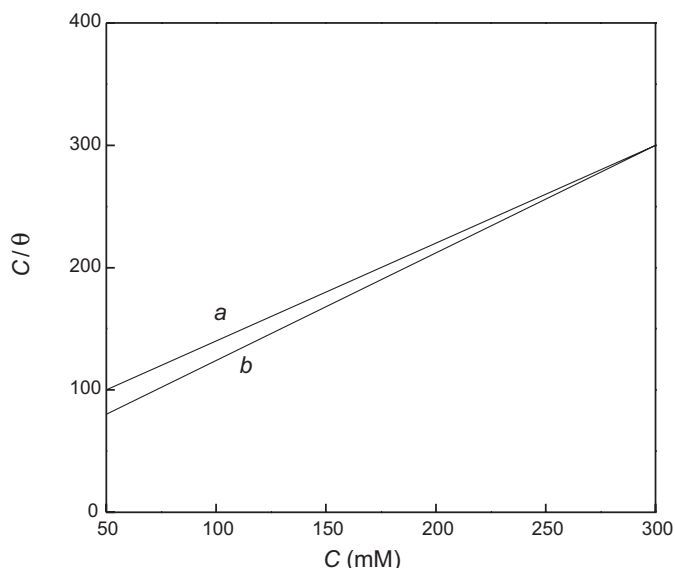
cules. The steel electrode is corroding uniformly and the corrosion rate in the absence of inhibitors is representative of the total number of corroding sites. Therefore, the corrosion rate in the presence of inhibitors may be assumed to represent the number of potentially corroding sites that remain after blockage because of inhibitor adsorption.

The surface coverage suggests that a chemical bond is formed between the metal atoms and the inhibitor molecules. The surface coverage is the function of the electronic density of the functional atom of the organic inhibitor; the molecules may be adsorbed on the metal–solution interface by the formation of either electrostatic or covalent bonds between the adsorbates and the metal surface atoms. Surface coverage data (θ) was used in determining inhibitor adsorption characteristics, which resulted in fitting the data to different isotherm type models, including Frumkin, Temkin, and Langmuir.

The simplest adsorption isotherm, the Langmuir isotherm, is based on the assumption that all adsorption sites are equivalent and that particle binding occurs independently from nearby sites, whether occupied or not. The degree of

Fig. 6. Langmuir's adsorption isotherm for carbon steel in HCl with inhibitors, (*a*) CTAB alone and (*b*) CTAB with 20 mmol/L OPD.

Fig. 7. Plots of hydrogen permeation current against time for carbon steel in HCl with CTAB and OPD inhibitors. (*a*) 1 mol/L HCl, (*b*) 1 mol/L HCl with 200 mmol/L CTAB, and (*c*) 1 mol/L HCl with 200 mmol/L CTAB and 20 mmol/L OPD.


surface coverage (θ) for different concentrations of the inhibitor in 1 mol/L HCl has been evaluated from weight loss measurements. The plot of C/θ against C yields a straight line (Fig. 6), clearly suggesting that the inhibitors obey Langmuir's adsorption isotherm.

Hydrogen permeation studies

Plots of hydrogen permeation current vs. time for carbon steel in 1 mol/L HCl in the presence and absence of inhibitors are shown in Fig. 7.
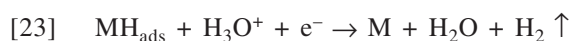
In acid solutions, hydrogen permeation through metals takes place in the following manner,

[21] $M + H_3O^+ + e^- \rightarrow H_2O + MH_{ads}$ (discharge step)
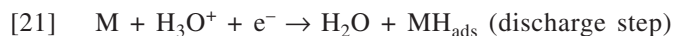
where M is the cathode metal surface, followed either by

[22] $MH_{ads} + MH_{ads} \rightarrow 2M + H_2 \uparrow$

or electrochemical desorption by

[23] $MH_{ads} + H_3O^+ + e^- \rightarrow M + H_2O + H_2 \uparrow$
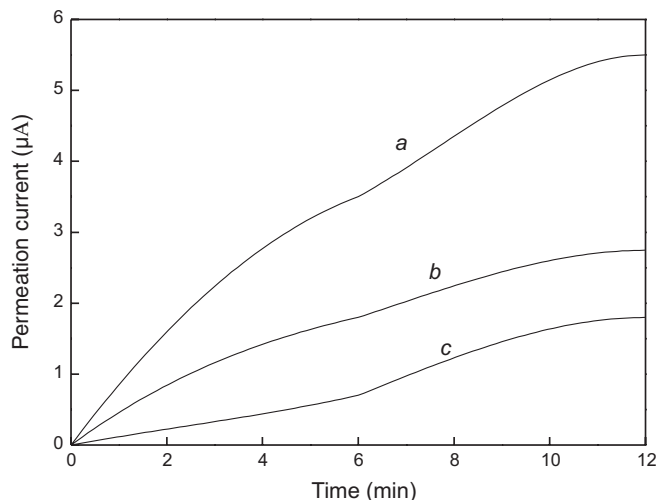
When the metal is immersed in acidic solutions, hydrogen gas is liberated on the steel surface. Some of the atomic hydrogen liberated during the process permeates through the metal (while the remainder is evolved as a fraction of the diffused hydrogen atoms – gas) and becomes occluded in the metal crystal lattice defects. The fraction of the diffused hydrogen atoms – gas that enters the metal produces some detrimental effects on the mechanical properties of steel, such as a decrease in ductility and loss of mechanical strength, leading to hydrogen embrittlement. Thus, the selection and design of inhibitors should take into account these detrimental effects. Inhibitors should either prevent hydrogen adsorption or favour H–H recombination.

The hydrogen permeation was controlled by the diffusion of hydrogen through the metal and the adsorption of the organic compound on the surface of the metal. The attainment of steady-state hydrogen permeation current density indicated a stable hydrogen surface coverage on the cathodic side of the membrane and saturation of the hydrogen traps present in the metal and a stable hydrogen concentration within the metal. The organic compounds were investigated for their ability to inhibit the rate at which hydrogen permeates through carbon steel in 1 mol/L HCl.
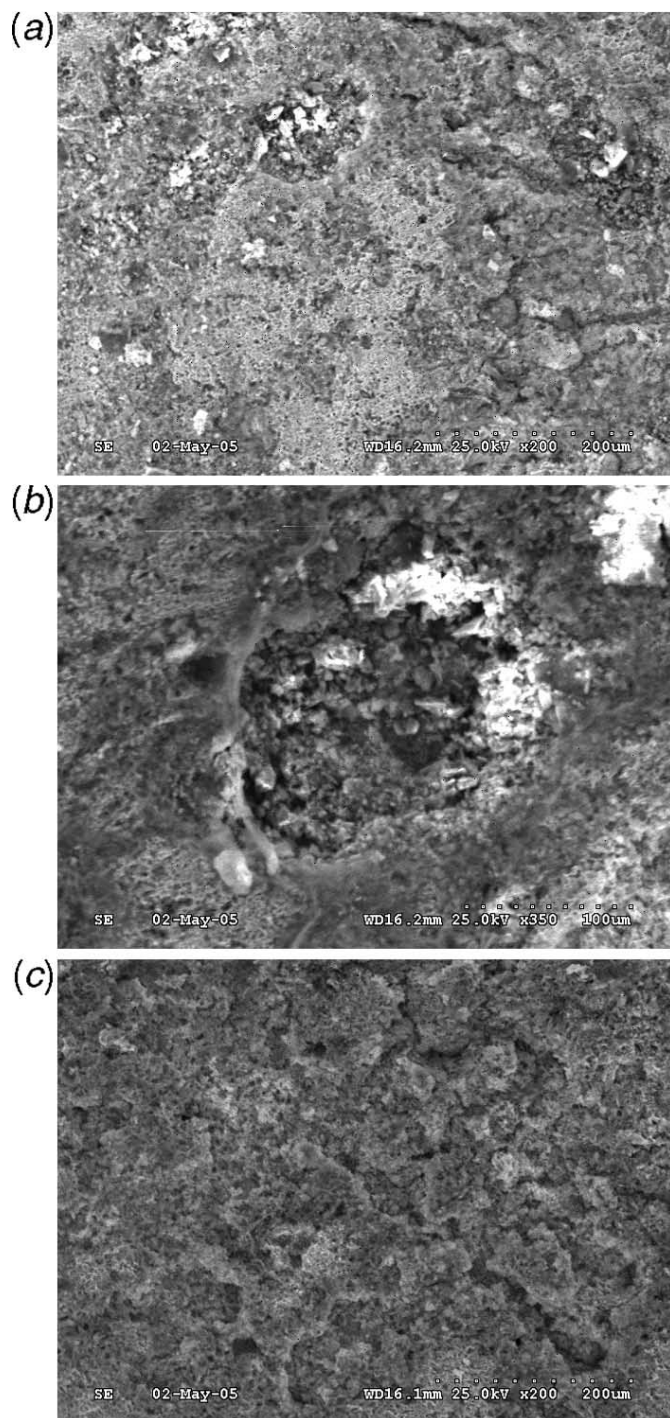
The transient curve shown in Fig. 7 for hydrogen permeation was controlled by the diffusion of hydrogen through the metal and the adsorption of the organic compound on the surface of the metal. The addition of CTAB alone reduces the permeation current compared with the blank. A further slight reduction in the permeation current was achieved by the addition of 20 mmol/L OPD with CTAB. This corresponds to higher IE values of the inhibitors and lesser permeation of hydrogen through the metal. It is expected that a system that induces maximum cathodic polarization will show lesser permeation current. Hence, CTAB with OPD exhibited a reduced permeation current.

The organic compounds possess high IE and, in addition, they reduce hydrogen permeation through the metal. This is to be expected since hydrogen arises from a corrosion reaction and any inhibition of this will necessarily lead to reduced hydrogen production and, therefore, reduced hydrogen uptake by the metal.

Scanning electron microscopy

Micrographs were made of carbon steel specimens in 1 mol/L HCl in the presence and absence of inhibitors and are shown in Figs. 8 and 9. The morphology of the specimen surface shows a characteristic corrosion pitting of mild steel in hydrochloric acid. These areas are highly oxidized. It was found that an uncovered surface of mild steel in acid corroded severely. Deep pits were observed throughout the specimen surface, which was immersed in HCl only, as clearly shown in Figs. 8*a*–8*c*. There was less pit formation in Fig. 9, which was made with CTAB alone in HCl. The addition of CTAB and OPD in HCl controlled the formation of

Fig. 8. SEM photographs for carbon steel dipped in 1 mol/L HCl.

Fig. 9. SEM photograph for carbon steel dipped in 1 mol/L HCl with 200 mmol/L CTAB.

Fig. 10. SEM photograph for carbon steel dipped in 1 mol/L HCl with 200 mmol/L CTAB and 20 mmol/L OPD.
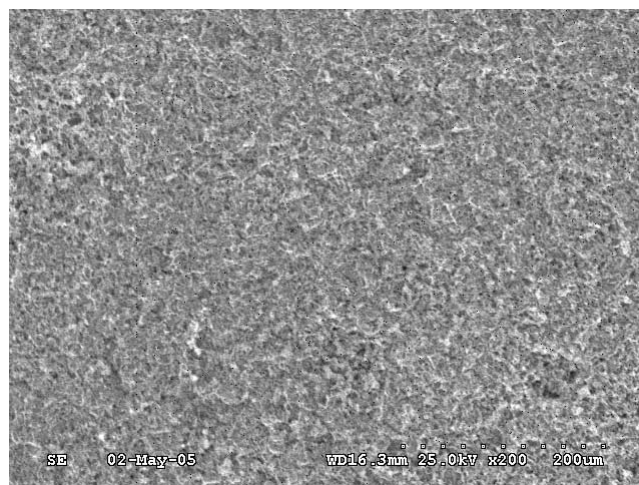

pits and protected the carbon steel from corrosion as shown in Fig. 10. These figures clearly show that the corrosion was less pronounced in the presence of inhibitors.

The increase in IE in all the techniques can be explained in the following way. Inhibition of corrosion can be attributed to the strong adsorption of the compound on the metal surface by the electron transfer from the organic molecule to the metal surface to form a coordinate type of link. This process is facilitated by the presence of low-energy vacant electron orbitals present in iron, as observed in the metals of the transition group.

As far as the inhibition process is concerned, it is generally assumed that the adsorption of the inhibitors at the metal solution interface is the first step in the action mechanism of inhibitors in aggressive acid media. Inhibition of corrosion of mild steel in HCl solution by the inhibitors can be explained on the basis of adsorption. Four types of adsorption may take place involving organic molecules at the metal solution interface: (*i*) electrostatic attraction between charged molecules and the charged metal, (*ii*) interaction of unshared electron pairs in the molecule with the metal, (*iii*) interaction of π electrons with the metal, and (*iv*) a combination of the above. It is apparent that the adsorption of these organic inhibitors on the metal surface could occur directly on the basis of donor acceptor interaction. Moreover, the presence of inhibitors in the organic structures makes the

formation of $d\pi$–$d\pi$ bond which enhances the adsorption of the compounds on the metal surface. These compounds inhibit the corrosion by controlling both the anodic and cathodic reactions. In an acidic solution, these compounds can exist as protonated species. These protonated species may adsorb on the cathodic sites of the mild steel surface and decrease the evolution of hydrogen. The adsorption of these compounds on anodic sites may decrease anodic dissolution of mild steel.

The formation of positively charged species in an acidic medium also facilitates the adsorption of the compound on the metal surface through electrostatic interactions between the organic molecule and the metal surface. Adsorbed molecules of the organic compound decrease the anodic and cathode reaction sites, resulting in a decrease in the active surface area, an increase in polarization resistance R_p, and a decrease in the rate of diffusion of ions to or from the metal surface. In addition, the organic compound may react with adsorbed corrosion intermediates of the steel forming products that passivate the steel surface. This indicates an increase in the energy barrier for proton discharge, leading to less gas evolution.

The mechanism of inhibition in CTAB may be attributed to the the micelles that are formed at these concentrations of CTAB, a cationic surfactant. Above a certain concentration range, these surfactant molecules aggregate in aqueous solution to form particles of colloidal dimensions called micelles. At concentrations of less than 100 mmol/L, CTAB does not effectively inhibit corrosion. However, it shows excellent corrosion inhibition properties at concentrations greater than 100 ppm. This is due to the fact that the micelle concentration takes place over a narrow range of surfactant concentration, the critical micelle concentration, and is accompanied by distinct changes in various physical properties such as surface tension, light scattering, electrical conductivity, solubility capacity, viscosity, and osmotic pressure for a wide variety of solutes. Below and up to the critical micelle concentration, the monomeric surfactant acts as a strong electrolyte, fully dissociated and aggregated. Aggregation begins at the critical concentration, at first with the formation of relatively small micelles that grow rapidly over a very limited concentration range to a size, which for a given surfactant remains approximately constant with further increase in surfactant concentration. Micelles are pictured as liquidlike, spherical in shape, their interior approximating that of liquid hydrocarbons but with hydrophilic end chains constrained to micelle surface. Above the critical micelle concentration, increases in the surfactant concentration lead to an increase in the number of micelles with little, if any, increase in the number of monomer surfactants (23).

With the hydrocarbon chains forming the inner hydrophilic core of the spherical micelles, the polar head groups of ionic micelles align together in a compact manner at the micelle surface. The ionic head groups of the surfactants and a portion of the counter ions form a compact "Stern" layer at the micelle surface at which about 60%–75% of the micelle charge is believed to be neutralized. The remaining ions form a diffuse Guoy–Chapman layer (24).

The addition of OPD in CTAB increases the IE in all the tests and this is due to adsorption of amines through electrostatic interaction between the positively charged amine and the negatively charged metal surface. In addition, in the case of aromatic amines the π electron interaction between the aromatic molecules and the positively charged metals may also play a role.

The concentration of inhibitor has a very great influence on the corrosion of carbon steel. This may be due to the formation of Fe^{2+} and Fe^{3+} complex species with ions like OH^- and Cl^-. For example, Fe^{2+} and Fe^{3+} ions formed from the metal dissolution should be able to form a corrosion product but the film of inhibitor on the surface prevents them. At low concentrations of these additives, the Fe^{2+} and Fe^{3+} ions resulting from metal dissolution should have formed an insoluble protective film of the type $Fe(OH)_3 - FeCl_3$ on the steel surface, but this is converted to a soluble one only at higher currents and temperatures.

The strong influence of the H^+ ion in this medium also helps in the oxidation of Fe^{++}. On the other hand, the solubility of a protective $Fe(OH)_3 - FeCl_3$ film is able to incorporate the inhibitor molecules to form a protective stable film. This incorporation of inhibitor molecules in the protective layer stabilizes the protective layer on the steel surface and decreases the corrosion rate.

Conclusions

The following conclusions can be made: (*i*) the IE calculated by gravimetric and potentiodynamic methods revealed that the combined inhibition effect of OPD and CTAB is better than the CTAB alone; (*ii*) potentiodynamic polarization data showed that the values of E_{corr} decreased using CTAB alone and decreased further with the addition of OPD; (*iii*) CTAB and OPD influence the b_c values but not specific changes in b_a values, showing that inhibitors are of mixed type; (*iv*) the R_p values obtained from EIS studies showed that the addition of OPD in CTAB increases R_p values; (*v*) the adsorption isotherm data showed that inhibitors obey Langmuir's adsorption isotherm; (*vi*) the IE was observed as high for 200 mmol/L of CTAB with 20 mmol/L of OPD in all the techniques studied; and (*vii*) micrographs clearly indicate that these inhibitors control the corrosion of carbon steel in 1 mol/L HCl.

Acknowledgement

References

1. A. Chetouani, A. Aouniti, B. Hammouti, N. Benchat, T. Benhadda, and S. Kertit. Corros. Sci. 45, 1675 (2003).
2. K. Tebbji, H. Oudda, B. Hammouti, M. Benkaddour, M. El Kodadi, F. Malek, and A. Ramdani. Appl. Surf. Sci. **241**, 326 (2005).
3. A. Dafali, B. Hammouti, R. Touzani, S. Kertit, A. Ramdani, and K. El Kacemi. Anti-Corros. Methods Mater. **49**, 96 (2002).
4. A. El-Ouafi, B. Hammouti, H. Oudda, S. Kertit, R. Touzani, and A. Ramdani. Anti-Corros. Methods Mater. **49**, 199 (2002).
5. K. Tebbji, H. Oudda, B. Hammouti, M. Benkaddour, M. El Kodadi, and A. Ramdani. Colloids Surf. A, **259**, 157 (2005).

6. M. Elayyachy, M. El Kodadi, B. Hammouti, A. Ramdani, and A. El Idrissi. Pigm. Resin Technol. **33**, 375 (2004).

7. A. Popova, E. Sokolova, S. Raicheva, and M. Chritov. Corros. Sci. **45**, 33 (2003).

8. H.-L. Wang, R.-B. Liu, and J. Xin. Corros. Sci. **46**, 10, 2455 (2004).

9. S. Bilgiç. Mater. Chem. Phys. **76**, 52 (2002).

10. Sk.A. Ali, M.T. Saeed, and S.U. Rahman. Corros. Sci. **45**, 253 (2003).

11. J. Cruz, R. Martínez, J. Genesca, and E. García-Ochoa. J. Electroanal. Chem. **566**, 111 (2004).

12. C.K. Emregül and O. Atakol. Mater. Chem. Phys. **83**, 373 (2004).

13. S.S. Abd El Rehim, H.H. Hassan, and M.A. Amin. Mater. Chem. Phys. **78**, 337 (2003).

14. B. El Medí, B. Mernari, M. Trainsnel, F. Bentiss, and M. Lagrenée. Chem. Phys. **77**, 489 (2003).

15. M. El Azhar, M. Traisnel, B. Mernari, L. Gengembre, F. Bentiss, and M. Lagrenée. Appl. Surf. Sci. **185**, 197 (2002).

16. P. Morales-Gil, G. Negrón-Silva, M. Romero-Romo, C. Ángel-Chávez, and M. Polomar-Pardavé. Electrochim. Acta, **49**, 4733 (2004).

17. P. Manjula, S. Manonmani, P. Jayaram, and S. Rajendran. Anti-Corros. Methods Mater. **48**, 319 (2001).

18. B. Ramesh Babu and R. Holze. Br. Corros. J. **35**, 204 (2000).

19. M.E. Haque, A.R. Das, and S.P. Moulik. J. Phys. Chem. **99**, 14032 (1995).

20. P.K. Jana and S.P. Moulik. J. Phys. Chem. **95**, 9525 (1991).

21. A.A. Abdel Fattah, K.M. Atia, F.S. Ahmed, and M.I. Roushdy. Corr. Prev. Control, **33**, 67 (1986).

22. F.B. Growcock and W.W. Frenier. J. Electrochem. Soc. **135**, 817 (1988).

23. K.N. Srinivasan, M. Selvam, and S. Venkatakrishna Iyer. J. Appl. Electrochem. **23**, 358 (1993).

24. F.B. Growcock, V.P. Lopp, and R.J. Josinski. J. Electrochem. Soc. **135**, 823 (1988).